

Tuning machine learning hyperparameters in electrical tomography of masonry walls

Abstract. The article presents a proposal for the final optimisation of the parameters of machine learning models in tomographic applications. In the case under consideration, electrical impedance tomography (EIT) was used to illustrate the distribution of moisture inside the walls of buildings. The mentioned topic focuses on optimising hyperparameters of machine learning models to optimise the efficiency of capturing accurate tomographic pictures. In the EIT, machine learning models are used to transform input measurements into output images. It is called an inverse or ill-posed problem that is difficult to solve due to insufficient arguments. In machine learning, the correct selection of model hyperparameters plays a key role. Therefore, the optimisation of these hyperparameters has a direct impact on the quality of the reconstruction. This article presents examples of hyperparameter optimisation for regression models and classification models based on the example of the k -nearest neighbours. The above methods were used in the electrical tomography system, intended to monitor and visualise the distribution of moisture inside the walls of buildings and structures. The results acquired during the research confirmed the high quality of the proposed methods.

Streszczenie. W artykule przedstawiono propozycję optymalizacji (dostrajania) parametrów modeli uczenia maszynowego w aplikacjach tomograficznych. W omawianym przypadku do zobrazowania rozkładu wilgoci wewnątrz ścian budynków wykorzystano elektryczną tomografię impedancyjną (EIT). Wspomniany temat koncentruje się na optymalizacji hiperparametrów modeli uczenia maszynowego w celu optymalizacji generowania obrazów tomograficznych o wysokiej jakości. W EIT modele uczenia maszynowego są wykorzystywane do przekształcania pomiarów wejściowych w obrazy wyjściowe. Ma to związek z tzw. problemem odwrotnym lub źle postawionym, który jest trudny do rozwiązania z powodu niewystarczającej liczby argumentów. W uczeniu maszynowym kluczową rolę odgrywa prawidłowy dobór hiperparametrów modelu. Dlatego optymalizacja tych hiperparametrów ma bezpośredni wpływ na jakość rekonstrukcji. W artykule przedstawiono przykłady optymalizacji hiperparametrów dla modeli regresyjnych, a także dla modeli klasyfikacyjnych na przykładzie metody k -najbliższych sąsiadów. Powyższe metody zostały zastosowane w systemie tomografii elektrycznej, przeznaczonym do monitorowania i wizualizacji rozkładu wilgoci wewnątrz ścian budynków i budowli. Uzyskane w trakcie badań wyniki potwierdziły wysoką jakość proponowanych metod. (Dostrajanie hiperparametrów uczenia maszynowego w tomografii elektrycznej ścian murowanych).

Keywords: electrical tomography; machine learning; moisture inspection; dump walls.

Słowa kluczowe: tomografia elektryczna; uczenie maszynowe; wykrywanie wilgoci; zawilgocenia murów.

Introduction

Damp building walls are the source of several health, construction, financial, and aesthetic issues. Damp, porous walls can be a breeding ground for bacteria, fungi, and pathogenic microorganisms that cause allergies and respiratory disorders in humans [1,2]. The water in the soil carries substances that seep into the foundations of buildings, diminishing their strength. Paint coatings typically peel off moist walls, causing browning and stains, as well as evident unattractive fungi, necessitating costly restorations [3].

Buildings, particularly ancient ones, are outfitted with modern monitoring systems due to the potential hazard to human and animal life posed by wet buildings [4]. Monitoring the moisture content of the walls of buildings of high historical significance entails both direct observation and the use of electrical instruments [5,6]. Electronic systems enable to read the parameters of particular probes and sensors positioned at various spots throughout the building. The downside of such conventional monitoring systems is that the measurements are only taken locally. As a result, the humidity readings provided by the individual measuring probes do not provide a complete cross-section of the tested wall's interior. Only tomographic technologies allow for the depiction of a cross-section of a spatial image of the interior of building walls. This circumstance became the primary impetus for dealing with this subject.

Machine learning technologies have grown in prominence in recent years. These techniques are also employed in tomography. Their primary goal is to solve the inverse issue related to the requirement to visualise the conductivity value of individual finite elements in the tested wall's cross-sectional mesh. Machine learning algorithms

are utilised in this case to convert input measurements into tomographic images. The measurement set in electrical tomography contains some arbitrary units that correlate with the voltages obtained at the various electrode pairs. The output values are also some arbitrary real-number units. These characteristics should not be confused with leadership. These are numerical values that are related to electrical conductivity. Each pixel of the finite element array (output image) in the specified model is assigned precise numerical values transformed into colours. Appropriate calibration, i.e. altering the colour scale, enables identifying moisture and other irregularities buried inside the building wall more accessible. Thus, it is possible to gain a cross-sectional or spatial image of the wall's interior using electrical tomography and electrodes placed on the surface of the wall being examined.

The concept of optimising the reconstruction process in electrical impedance tomography is presented in this study (EIT). The novel strategy consists of mixing different machine learning approaches so that the best one of them can be chosen [7]. Furthermore, different prediction models are trained for each pixel of the tomographic picture, allowing the ideal approach for a given pixel to be selected while considering a specific measurement vector. Thus, it increases the method's versatility, and while it requires training an additional classification predictor, the consequent improvement in image quality justifies the tomographic system's increased computing complexity [8]. Furthermore, the linear regression models and the kNN classifier are fine-tuned for fitness function selection and optimisation.

Several machine learning approaches, including Elastic Net, linear regression (LR), and Artificial Neural Networks,

were applied in the study (ANN). When the novel concept was compared to popular approaches, it was discovered that thanks to pixel-oriented hybrid learning, the new approach's reconstructions are superior to those obtained with standard methods. The authors' key contribution is the creation of the notion of dynamic selection of the optimal reconstruction method, which works independently for each image pixel. Furthermore, the algorithms use the k-nearest neighbours technique to improve the learner selection for linear regression and the distance function selection for the classifier. The new method employs hybrid learning and makes better use of PC power to improve imaging accuracy.

Materials and Methods

A finite element mesh of a spatial (3D) wall segment was created based on measurements taken in a historical building. A simulation model was created using the Eiders toolbox [9,10] to generate learning instances for training machine learning models. It resulted in 30,000 impedance tomography training cases (EIT). The measuring apparatus is outfitted with a 16-electrode measuring system. The measurement vector has 448 values that are connected to voltage dips. The reconstructed image has a resolution (number of pixels) of 10752 pixels. The actual model of the tested piece of the building wall is depicted in Figure 1. Figures 1(a, b, and c) depict the test stand, the proximity of the electrodes to the wall, and the internal structure of the electrode, in that order. The algorithmic model's validation was carried out in a laboratory setting.

The electrodes are spaced by 40 cm on two metal strips. Each strip has 16 electrodes, for a total of 32 electrodes. The model also incorporates an electrical impedance tomography (EIT), which generates an electric current with defined parameters (voltage, current, frequency, and amplitude) for switching electrode pairs. The voltages between the separate electrodes are read by the tomograph and sent to the output port. In addition, a structured data transfer protocol allows data to be transferred to other modules and processed further [11-13].

To train machine learned models, simulated training data sets were prepared, as previously stated. The training data was generated using the generalised finite element approach included in the Eiders toolbox [9].



Fig. 1. EIT test stand: (a) - measurement site, (b) - electrode approach, (c) - electrode structure.

Figure 2a depicts the procedure for developing a simulation measurement scenario. First, on the finite element mesh, a model of the moist part of the wall is constructed. The forward problem is then addressed using the finite element approach, which allows the measurement voltage vector (arbitrary units) to be assigned to the distribution of the material conductivity coefficients (Figure 2b).

The necessity to overcome the so-called reverse problem is the main obstacle in electrical tomography. It is also a misplaced problem because the mathematical model contains fewer arguments (measurements, inputs) than the required number of outputs (image pixels). This research aims to create a 10752-pixel spatial moisture image from a vector of 448 data. To reduce the complexity level of generating multi-finite element graphics, single models with 448 values for input and only one pixel for output are trained (448-model-1).

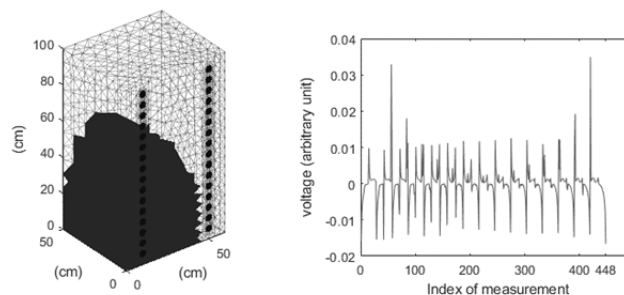


Fig. 2. Creating simulation measurements: (a) - reference image on a mesh, (b) - values of the measurement vector.

Figure 3 depicts the pixel-oriented hybrid approach concept. According to the novel hybrid method's concept, the number of created models is equal to the total number of pixels (finite elements) in the cross-sectional grid, which is 10752. As a result, colour values for several different pixels can be generated using the same input values. It is feasible because, when training the predictive model, each model uses a different set of coefficients, parameters, and hyperparameters on which the process of transforming input values to output values is dependent. It is clear that when several different homogeneous methods are used for a specific measurement case (e.g., linear regression with the learning least-squares method LR-LS, linear regression with the learning machine support vector LR-SVM, artificial neural networks ANN, elastic network, LARS, etc.), the results are not equally good.

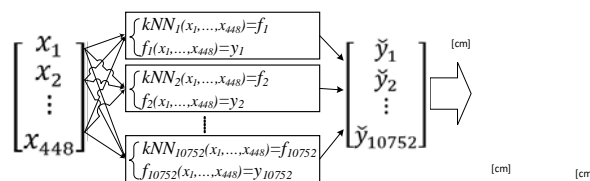


Fig. 3. The pixel-oriented hybrid method's concept.

One of the approaches is usually superior to the others, depending on the test object and even the measurement circumstance. Furthermore, if we go one step further and decrease the assumption above from the measurement case for all pixels of the reconstruction image to the value of a single-pixel in a specific measurement instance, we get the method described in this study. After training multiple models (elastic net, LR-LS, LR-SVM, and ANN), you must choose which model provides the best reconstruction for a given pixel. As a result, the hybrid technique also assumes building a classification model with as many classes as previously trained homogeneous methods (in our case, these are 3 methods: elastic net, LR and ANN). The classification model was trained on the identical 448-element input vectors using the k-nearest neighbours (kNN) approach. The kNN model, like regression models,

classifies classes (outputs) based on both the measurement vector and the number of pixels due to proper hyperparameter estimation.

By selecting a more effective learner, the algorithm utilised optimises the linear regression model. There are two types of learners to pick from least squares and support vector machines (SVM). The Linear Regression (LR) model employs a learner based on the reconstructed pixel and the input data to produce better outcomes. Linear regression (LR) and support vector machines (SVM) are used in the LR-SVM technique. The algorithm has been optimised for the 448-element input data vector. The absolute contraction and selection operator (LASSO) employs the L1 regularisation technique, employing a regression model that adds the "absolute magnitude" of the coefficient as a penalty component to the loss function. A linear regression model based on the SVM approach was used as a learner. The linear regression model's loss function is given by the formula $f(x) = x\beta + b$, where x is an observation of p predictor variables, is a vector of p coefficients, and b is a bias. The mean square error (MSE) is calculated as a loss function in the implemented algorithm and takes the form $\ell[y, f(x)] = \max[0, |y - f(x)| - \varepsilon]$ where $y \in (-\infty, \infty)$ is the reconstruction of the response value. The least absolute shrinkage and selection operator (LASSO) cost function is depicted in $\min_{\beta_0, \beta} \left(\frac{\sum_{i=1}^n (y_i - b - x_i^T \beta)^2}{2n} + \lambda \sum_{j=1}^p |\beta_j| \right)$ where x_i^T is a transposed vector of length p in observation i , n is the number of observations, y_i is a pixel reconstruction in observation i and λ is a non-negative regularisation parameter. In this study $\lambda = \frac{1}{n}$, b is a scalar deviation, and β is a vector of length p . As λ rises, the number of non-zero parameters β declines.

Regulated support vector machines (SVM) and least squares regression are included in LR-SVM. The model employs stochastic gradient descent to minimise the objective function. The described method employs SVM with ridge penalty and optimises SVM using double SGD.

Figure 4 depicts the response area for a case and image pixel chosen at random. The blue dots show the 30 iterations that the method takes to maximise learner selection in linear regression. The red diamond represents the minimum objective function. The SVM technique was revealed to be the chosen learner in the presented scenario.

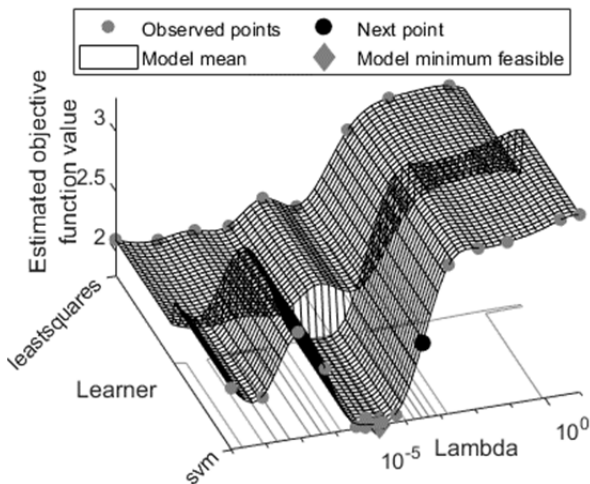


Fig. 4. Objective function model (linear regression with least squares or SVM learner) for a randomly selected pixel.

The overall computation time for the 30 iterations depicted in Figure 4 30.1957 seconds. The objective function's total evaluation time is $t = 12.8269$ seconds. SVM with $\lambda = 1.370210$ appeared to be the better learner for the best observed feasible point (-5). The observed objective function value $f(x)$ is 1.7843, while the estimated objective function value is 1.7977. The time it took to evaluate the function was 0.30455 seconds.

Figure 5 depicts the objective function values achieved after sequential computation stages. The calculated minimum target line resembles a hyperbola, as can be seen. It demonstrates that the optimisation process is on the right track.

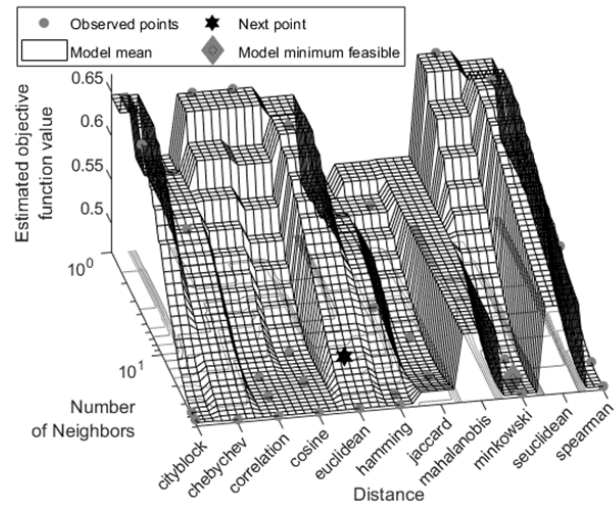


Fig. 6. Objective function in the kNN model for a randomly selected pixel
Fig. 7.

The response surface generated during the kNN classifier optimisation procedure is depicted in Figure 5. The algorithm's task is to choose one of the eleven distance functions.

The optimisation result in the investigated situation was the use of the Minkowski method, which was satisfied by

formula $d_m = \sqrt[p]{\sum_{j=1}^n |x_{sj} - y_{tj}|^p}$ where d_m is the distance,

x_s denotes the input vector, and y_t denotes the output vector. The Minkowski distance yields the city block distance in the particular situation of $p = 1$. The Euclidean distance is given by function d_m for the particular case of $p = 2$. The Chebychev distance is given by the d_m distance in the specific situation of $p = \infty$. The overall computation time for the 30 iterations depicted in Figure 6 (blue dots) was 17.7 seconds. The objective function took 1.3 seconds to evaluate in total. The observed objective function value for the best observed possible point was 0.47, the estimated objective function value was 0.46995, and the function evaluation time was 0.040271. The estimated objective function value for the best estimated feasible point was 0.46995, and the function evaluation time was 0.040863.

Results

Figure 6 depicts two test cases used to validate the provided approach. The reference images are located in the first column (Pattern). The images in the following three columns were generated using Elastic Net, linear regression, and ANN, in that order. The final column displays the images produced by the new hybrid approach.

Figure 6 corresponds to Table 1. It gives a study of the produced reconstructions based on three indicators: mean

squared error, mean squared error, and mean squared error plus mean squared error plus mean squared error (MSE), relative image error (RIE), and image correlation coefficient (ICC). The ICC function, also known as the Pearson correlation coefficient. There are two reconstructions with varying moisture levels. The disadvantage of subjectivism constantly hampers visual evaluation of reconstruction. As a result, it can be used in addition to the objective assessment based on MSE, RIE, and ICC metrics. Nonetheless, the reconstructions obtained by the pixel-dependent hybrid technique are the best.

The last column in Table 1 displays the average values of the MSE, RIE, and ICC indicators for all investigated cases. The final three lines of the table demonstrate the unambiguous comparison of the metrics for the Elastic Net, LR, and ANN with the new hybrid pixel dependent selection method. In all comparisons, the novel hybrid idea produced the greatest quality reconstructive images.

Conclusions

A new concept, pixel-dependent hybrid EIT system, was suggested in this study. The idea is that the quality of the restored pixels is determined by the reconstruction method utilised. Three machine learning algorithms (Elastic Net, LR, and ANN) were trained to validate the preceding statement. Four test cases were also rebuilt utilising a new hybrid concept (see Figure 7 and Table 1). Fine-tuning, which is used in various machine learning methods, is a critical component of the new methodology. The learner in the linear regression model was optimised by using the least-squares or SVM function. The best distance function was chosen for the kNN classifier. The results were compared to those obtained using homogeneous component techniques. According to the quantitative evaluation of the MSE, RIE, and ICC indices, the new pixel-dependent hybrid technique is the most effective. It is preferable to use a single

Table 1. Comparison of image reconstructions

Methods	Evaluation metrics	Investigated cases		Average
		#1	#2	
ANN	MSE	31.084	3.593	17.33
	RIE	0.893	0.827	0.86
	ICC	0.801	0.479	0.64
LR-LS	MSE	4.709	3.393	4.05
	RIE	0.347	0.804	0.57
	ICC	0.868	0.288	0.57
LR-SVM	MSE	5.078	2.958	4.01
	RIE	0.361	0.751	0.55
	ICC	0.857	0.476	0.66
New hybrid concept (NHC)	MSE	0.174	0.928	0.55
	RIE	0.066	0.420	0.24
	ICC	0.995	0.918	0.95
Is MSE for NHC the smallest?		YES	YES	YES
Is RIE for NHC the smallest?		YES	YES	YES
Is ICC for NHC closest to 1?		YES	YES	YES

homogeneous approach for all pixels in the rebuilt image.

Authors: Tomasz Rymarczyk, Prof. Eng., University of Economics and Innovation, Projektowa 4, Lublin, Poland, E-mail: tomasz.rymarczyk@netrix.com.pl; Grzegorz Kłosowski, Ph.D. Eng., Lublin University of Technology, Nadbystrzycka 38A, Lublin, Poland, E-mail: g.klosowski@pollub.pl; Paweł Rymarczyk, M.Sc. Eng., Research and Development Center Netrix S.A., Wojciechowska 31, Lublin, Poland, E-mail: pawel.rymarczyk@netrix.com.pl; Jan Sikora, Prof. Eng., Lublin University of Economics and Innovation, Projektowa 4, Lublin, Poland, E-mail: jan.sikora@wsei.lublin.pl; Przemysław Adamkiewicz, Ph.D., Lublin University of Economics and Innovation, Projektowa 4, Lublin, Poland, E-mail: przemyslaw.adamkiewicz@wsei.lublin.pl; Michał Oleszek, M.Sc. Eng., Research and Development Center Netrix S.A., Wojciechowska 31, Lublin, Poland, E-mail: michal.oleszek@netrix.com.pl.

REFERENCES

- [1] Rymarczyk T., Kłosowski G., Hoła A., Sikora J., Wołowicz T., Tchórzewski P., Skowron S., Comparison of Machine Learning Methods in Electrical Tomography for Detecting Moisture in Building Walls. *Energies*, 14 (2021), 2777, doi:10.3390/en14102777.
- [2] Hoła A., Sadowski Ł., Non-destructive in situ identification of the moisture content in saline brick walls using artificial neural networks. In *Proceedings of the Creative Construction Conference 2019*, (2019), 77–82.
- [3] Surowska B., Majerski K., Bieniaś J., Kłosowski G., Mechanical behaviour of hygrothermal conditioned fiber metal laminates. In *Proceedings of the 16th European Conference on Composite Materials, ECCM 2014*, (2014), 1–3.
- [4] Rymarczyk T., Kłosowski G., Hoła A., Hoła J., Sikora J., Tchórzewski P., Skowron Ł., Historical Buildings Dampness Analysis Using Electrical Tomography and Machine Learning Algorithms. *Energies*, 14 (2021), 1307, doi:10.3390/en14051307.
- [5] Szczesny A., Korzeniewska E., Selection of the method for the earthing resistance measurement, *Przegląd Elektrotechniczny*, 94 (2018), 178–181.
- [6] Duraj A., Korzeniewska E., Krawczyk A., Classification algorithms to identify changes in resistance. *Przegląd Elektrotechniczny*, 1 (2015), 82–84, doi:10.15199/48.2015.12.19.
- [7] Mikulka J., GPU-Accelerated Reconstruction of T2 Maps in Magnetic Resonance Imaging. *Meas. Sci. Rev.*, 15 (2015), 210–218, doi:10.1515/msr-2015-0029.
- [8] Majchrowicz M., Kapusta P., Jackowska-Strumiłło L., Sankowski D., Acceleration of image reconstruction process in the electrical capacitance tomography 3D in heterogeneous, multi-GPU system. *Informatics Control Meas. Econ. Environ. Prot.*, 7 (2017), 37–41, doi:10.5604/01.3001.0010.4579.
- [9] Adler A., Lionheart W.R.B., Uses and abuses of EIDORS: an extensible software base for EIT. *Physiol. Meas.*, 27 (2006), 25–42, doi:10.1088/0967-3334/27/5/S03
- [10] Kryszyn J., Smolik W., Toolbox for 3D modelling and image reconstruction in electrical capacitance tomography. *Informatics Control Meas. Econ. Environ. Prot.* (2017), No. 7, 137–145, doi:10.5604/01.3001.0010.4603
- [11] Porzuczek J., Assessment of the Spatial Distribution of Moisture Content in Granular Material Using Electrical Impedance Tomography. *Sensors*, 19 (2019), 2807, doi:10.3390/s19122807
- [12] Rymarczyk T., New Methods to Determine Moisture Areas by Electrical Impedance Tomography, *International Journal of Applied Electromagnetics and Mechanics*, 52 (2016), 79–87
- [13] Rymarczyk T., Filipowicz S.F., Measurement Methods and Image Reconstruction in Electrical Impedance Tomography. *Przegląd Elektrotechniczny*, 88 (2012), No.6, 247–250